

Interlinking Au nanoparticles in 2D arrays via conjugated dithiolated molecules

Jianhui Liao¹, Markus A Mangold¹, Sergio Grunder²,
Marcel Mayor^{2,3,4}, Christian Schönenberger¹
and Michel Calame^{1,4}

¹ Department of Physics, University of Basel, Klingelbergstrasse 82,
CH-4056, Basel, Switzerland

² Department of Chemistry, University of Basel, St Johannis-Ring 19,
CH-4056 Basel, Switzerland

³ Forschungszentrum Karlsruhe GmbH, Institute for Nanotechnology,
PO Box 3640, D-78021 Karlsruhe, Germany

E-mail: Marcel.Mayor@unibas.ch and Michel.Calame@unibas.ch

New Journal of Physics **10** (2008) 065019 (7pp)

Received 20 February 2008

Published 30 June 2008

Online at <http://www.njp.org/>

doi:10.1088/1367-2630/10/6/065019

Abstract. We investigate the importance of anchoring end-groups in conjugated oligomers for the formation of molecular junction networks. Oligo(phenylene ethynylene) with a single (OPE-MT) and two (OPE-DT) thiol end-groups have been inserted into self-assembled octanethiol-capped gold nanoparticle arrays by taking advantage of molecular exchange. Comparing the exchange for tens of devices, we observe significantly different final conductances for devices comprising monothiol- and dithiolated compounds. Our experimental results support the picture that OPE-DT covalently bridge neighboring nanoparticles via Au-S bonds at both ends of the conjugated oligomer to form interlinked networks of molecular junctions.

⁴ Author to whom any correspondence should be addressed.

Contents

1. Introduction	2
2. Experimental methods	2
3. Results and discussion	3
4. Conclusion	6
Acknowledgments	6
References	6

1. Introduction

The perspective of using single organic molecules as electronic components in circuits has driven the development of many techniques to investigate the electronic transport properties of single or few molecules [1]–[3]. We have recently demonstrated that two-dimensional (2D)-nanoparticle arrays represent a suitable platform to build a large number of molecular junctions [4]. Starting from an array stabilized via alkanethiols, we showed that the conductance through the array increases dramatically after inserting conjugated oligomers via molecular exchange. Optical spectroscopy also confirmed the insertion of the conjugated compounds within the arrays [5]. The 2D-nanoparticle arrays therefore represent an interesting test bed for molecular electronics since they are stable at room temperature in air, enabling the formation of robust molecular junctions, and can resist common organic solvents. It is however delicate to gain insight into the details of the junction formation.

Using oligo(phenylene ethynylene) (OPE) as a model molecular system, we investigate here the differences emerging upon exchange of single thiolated OPE (OPE-MT) and dithiolated OPE (OPE-DT). The conjugated oligomers were inserted into octanethiol-capped nanoparticle arrays by place-exchange and the conductance of the arrays was measured before and after exchange. We find that there are significant differences in the behavior of OPE-MT and OPE-DT and provide strong evidence that OPE-DT is best suited to form molecular junction networks by interlinking neighboring nanoparticles via Au–S bonds at both ends of the molecular compound.

2. Experimental methods

Gold colloidal particles with 10 nm diameter were synthesized by reduction of hydro-tetrachloroaurate with trisodium citrate and tannic acid [4, 6]. The nanoparticles were transferred from water to ethanol by centrifugation and mixed with octanethiol molecules. Typically, 10 ml colloidal particles in ethanol were mixed with 200 μ l octanethiol. After 24 h, the nanoparticles were encapsulated by a monolayer of octanethiols and precipitated at the bottom of the container. Ethanol was used to wash the capped gold nanoparticles and remove octanethiol molecules in excess. Finally, the nanoparticles were dispersed in chloroform by ultrasonic treatment.

Patterned 2D nanoparticle arrays were prepared by a combination of self-assembly and micro-contact printing [4, 7, 8]. The solution of nanoparticles was spread on a convex water surface with a pipette. After evaporation of the solvent, octanethiol-capped gold nanoparticles

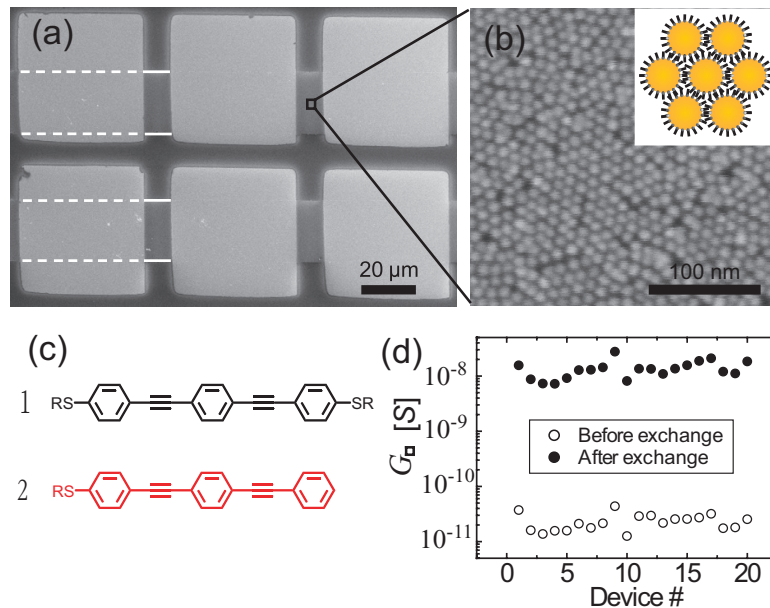


Figure 1. (a) SEM image of devices prepared by evaporation of metallic contact pads on top of printed nanoparticle monolayer lines. The white lines emphasize the edges of the stamped nanoparticles lines (dashed when below the contact pads). (b) High magnification SEM image showing the hexagonal arrangement of a nanoparticle array. Inset: schematic picture of alkanethiol-capped gold nanoparticles before exchange. (c) Conjugated oligomers studied. **1**: OPE-DT and **2**: OPE-MT. The compounds were synthesized in their acetyl-protected form ($R=\text{COCH}_3$). A deprotection step was carried out to form the free thiol for coordination with the Au nanoparticles ($R=\text{Au}$). (d) Sheet conductance of 20 devices measured before (\circ) and after (\bullet) molecular exchange of molecule **1**.

were self-assembled into 2D arrays at the air–water interface. Patterned poly-dimethylsiloxane (PDMS) stamps were used to transfer the 2D films from the water surface onto solid substrates (SiO_2/Si) and form nanoparticle monolayer lines. Afterwards, metallic contact pads (5 nm Ti + 45 nm Au) were evaporated on the top of these lines using a transmission electron microscopy (TEM) grid as shadow mask.

Place-exchange was used to introduce conjugated molecules into the arrays and partially replace the alkanethiols [9]–[11]. To achieve this, we immersed the sample in 1 mM solution of the incoming molecule in tetrahydrofuran (THF) with ammonium hydroxide as a deprotecting agent at 40°C under argon atmosphere. The sample was taken out of the solution after 10 h, rinsed with THF and dried with nitrogen gas. The dc conductance measurements were performed on a probe station in air at room temperature using an I–V converter.

3. Results and discussion

Figure 1(a) shows a scanning electron microscope (SEM) image of a typical sample. Hereafter, we will refer to a *sample* as the chip with printed and contacted lines of nanoparticle arrays. On the left side of figure 1(a), the edges of the printed lines are emphasized with a white line

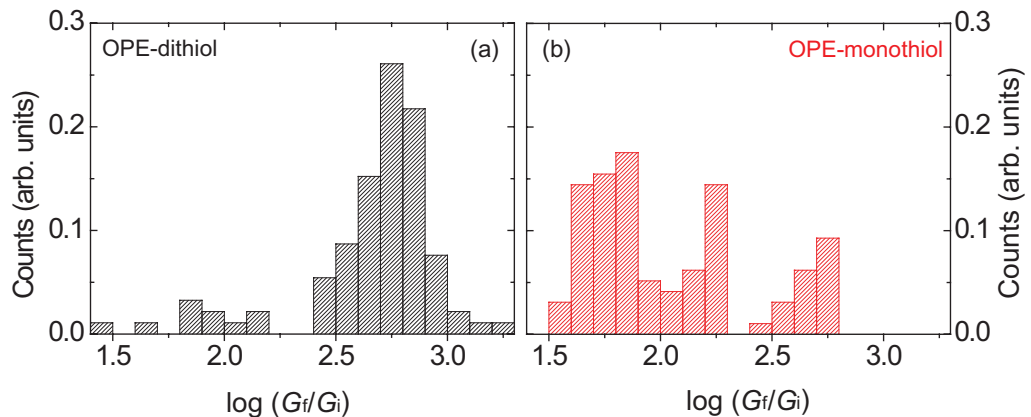


Figure 2. Histograms of $\log(G_f/G_i)$, where G_f is the final sheet conductance after exchange and G_i the initial conductance before exchange for OPE-DT (a) and OPE-MT (b).

(dashed when below the contact pads). Every pair of neighboring contact pads will be termed a *device* and contains typically 10^6 molecular junctions between the metallic contacts. One sample contains a few tens of devices. A higher magnification SEM image of the nanoparticle array between the metallic contacts is shown in figure 1(b). We observe a regular, hexagonal close-packed array with the nanoparticles distance determined by the capping octanethiols. The inset is a schematic view of the structure. The molecules investigated in this work are shown in figure 1(c). Molecules **1** (OPE-DT) and **2** (OPE-MT) have the same molecular core. Their only difference is the absence of a second acetyl-protected thiol anchoring group in molecule **2**. We prepared three samples for each compound and measured for all devices their initial conductance G_i before exchange and final conductance G_f after exchange. We measured 83 devices for OPE-DT and 60 devices for OPE-MT. Figure 1(d) shows the sheet conductance G_{\square} for 20 devices measured before and after exchange for OPE-DT. Here, $G_{\square} = G \cdot l/w$, where w is the width of the printed nanoparticle line, l the distance between the two neighboring contact pads and G the measured conductance. An increase in conductance by 2–3 orders of magnitude is observed, consistent with our previous observations [4]. In our experiments, we find that the initial conductance G_i of all devices is not always the same. This device-to-device fluctuation is apparent in figure 1(d). We attribute this effect to local geometrical variations emerging during sample preparation. Note, however, that the variation of the final conductance value G_f correlates very well with that of the G_i . This indicates that the structure of the arrays remains intact during the course of exchange, as also demonstrated by SEM images of the arrays taken before and after exchange [5]. Given this observation, we propose to compare the ratio of conductances G_f/G_i after and before exchange to investigate the differences emerging from the difference in anchoring groups between compounds **1** and **2**.

Figures 2(a) and (b) show the histograms of the logarithm of the conductance ratios (G_f/G_i) for OPE-DT and OPE-MT, respectively. We obtain average ratios of 600 for the former and 230 for the latter. These experimental results reveal first of all that a conductance increase is observed for both conjugated compounds. We also note that the increase is, on average, larger for OPE-DTs. Finally, we can observe a broader distribution of the conductance ratios for OPE-MTs than for OPE-DTs. To gain further insight, we can use a simple tunneling model [12]–[14] and extract the relative decay factors of the molecules. Here, the conductance

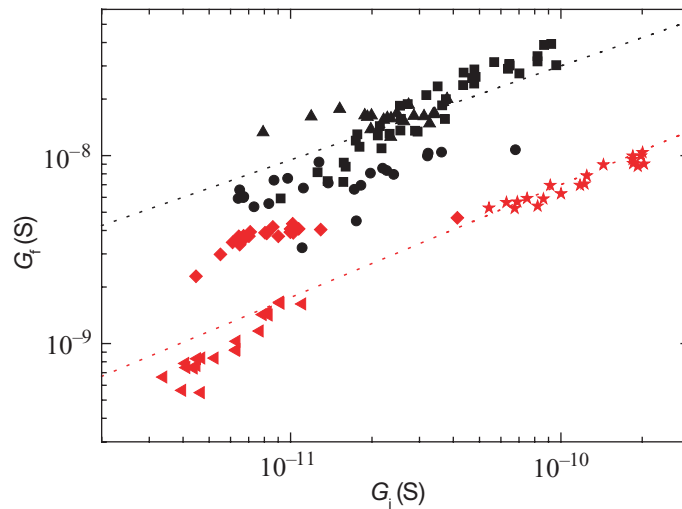


Figure 3. The log–log plot of the final conductance G_f as a function of the initial conductance G_i of all devices for OPE-DT molecules (black) and OPE-MT molecules (red). Different symbols indicate data from different samples. The dotted lines show the average slopes for both molecular compounds of 0.5 (dithiol) and 0.6 (monothiol).

is given by $G = G_c \cdot e^{-\beta d}$, where d is the molecule length and the decay factor β is determined by the molecule between the electrodes. The prefactor G_c accounts for the molecule–electrode contact conductance. As discussed previously, we anticipate that the structure of the arrays is preserved after molecular exchange. We can therefore assume that the inter-particle distance remains constant throughout the exchange and we can then relate G_f to G_i as follows:

$$\log G_f = \log G_{c,f} - (\beta_f/\beta_i) \log G_{c,i} + (\beta_f/\beta_i) \log G_i,$$

where $G_{c,i}$ and $G_{c,f}$ are the contact conductance before and after exchange, β_i and β_f the decay factors before and after exchange.

Figure 3 shows a log–log plot of G_f as a function of G_i for all devices measured. Black symbols indicate data for OPE-DT, while red symbols are for OPE-MT. The different symbol shapes represent different samples. From the slope, we can deduce the ratio of the two decay factors β_f/β_i . Linear fits to the data from each sample and for each compound allow us to calculate average slopes of 0.5 ± 0.2 for OPE-DT and 0.6 ± 0.2 for OPE-MT, taking into account the number of data points to weight the contribution from each sample. The dotted lines in figure 3 show these average slopes. Reported values of the decay factor for alkanethiols β_i range from 0.6 to 1.1 \AA^{-1} [15]–[17] whereas the values for OPE compounds β_f are between 0.21 and 0.57 \AA^{-1} [12], [18]–[21]. We can therefore expect a ratio of both the values between roughly 0.2 and 1.0 . Our values are well within this range. Note also that, since both the compounds have the same conjugated core, the slopes should be identical. We observe indeed very similar values.

The main difference between both the compounds in our results is evidenced by looking at figure 3 for a given initial conductance G_i . Fixing G_i translates in selecting a specific average interparticle distance as defined by the microscopic nanoparticle arrangement for the device considered. By looking at the conductance after exchange G_f for both the compounds at a given initial conductance G_i , we can therefore minimize the influence of structural differences

on the conductance of the arrays and achieve a robust comparison. The data show that, for any given initial conductance value, the final conductance of the arrays after insertion of the conjugated compounds is systematically larger for OPE-DTs (black) than for OPE-MTs (red), with only very few exceptions. Firstly, this reinforces the observation drawn from figure 2 that the average value of the ratio G_f/G_i is larger for OPE-DT (600) than for OPE-MT (230). Secondly, from the equation above, this means that the prefactors $G_{c,f}$ must be different for OPE-DT and OPE-MT since the ratio β_f/β_i is similar for both the molecules and $G_{c,i}$ is the same since the initial molecules are identical (alkanethiols). How can we interpret this observation? In the simple tunneling model considered, the prefactor G_c reflects the efficiency of charge transport across the contacts of the molecules to the Au electrodes (here, the nanoparticles), while the exponential decay accounts for non-resonant charge tunneling through the molecular core. In this picture, the absence of a covalent bond between molecule and electrode is expected to lead to a decrease in conductance [12, 14, 22]. Due to a reduced density of states at the molecule–metal interface, the conductance prefactor, which is proportional to the product of the density of states at both metal–molecule interfaces, will thus be reduced. We can therefore associate here the systematic lower conductance of molecular junctions formed by OPE-MT molecules with the absence of a metal–molecule covalent bond at one end of the molecule. These experiments therefore provide strong evidence that the place exchange of conjugated dithiolated compounds (OPE-DT) into a nanoparticle array leads to an interlinking of neighboring nanoparticles, resulting in the formation of a chemically interconnected network of molecular junctions.

4. Conclusion

We have compared the conductance of nanoparticle arrays after the insertion of conjugated oligomers with one or two thiol end-groups via place exchange. Arrays with dithiolated compounds not only exhibit a larger average conductance increase, but also systematically show a larger final conductance than arrays with monothiolated compounds, given a similar initial conductance before exchange. These observations strongly support the view that dithiolated oligomers interlink neighboring nanoparticles via chemical bonds upon exchange to form 2D networks of molecular junctions.

Acknowledgments

This work has been supported by the Swiss National Center of Competence in Research ‘Nanoscale Science’, the Swiss National Science Foundation, the Gebert-Rüf Foundation and the European Science Foundation via the Eurocore program on Self-Organized Nanostructures (SONS).

References

- [1] Mantooth B A and Weiss P S 2003 Fabrication, assembly, and characterization of molecular electronic components *Proc. IEEE* **91** 1785–802
- [2] Chen F, Hihath J, Huang Z, Li X and Tao N J 2007 Measurements of single-molecule conductance *Annu. Rev. Phys. Chem.* **58** 535–64
- [3] Lindsay S M and Ratner M A 2007 Molecular transport junctions: clearing mists *Adv. Mater.* **19** 23–31

- [4] Liao J, Bernard L, Langer M, Schönenberger C and Calame M 2006 Reversible formation of molecular junctions in 2d nanoparticle arrays *Adv. Mater.* **18** 2444–7
- [5] Bernard L, Kamdzhilov Y, Calame M, van der Molen S J, Liao J and Schönenberger C 2007 Spectroscopy of molecular junction networks obtained by place exchange in 2d nanoparticle arrays *J. Phys. Chem. C* **111** 18445–50
- [6] Tsutsui G, Huang S, Sakaue H, Shingubara S and Takahagi T 2001 Well-size-controlled colloidal gold nanoparticles dispersed in organic solvents *Japan. J. Appl. Phys.* **40** 346–9
- [7] Santhanam V and Andres R P 2004 Microcontact printing of uniform nanoparticle arrays *Nano Lett.* **4** 41–4
- [8] Santhanam V, Liu J, Agarwal R and Andres R P 2003 Self-assembly of uniform monolayer arrays of nanoparticles *Langmuir* **19** 7881–7
- [9] Song Y and Murray R W 2002 Dynamics and extent of ligand exchange depend on electronic charge of metal nanoparticles *J. Am. Chem. Soc.* **124** 7096–102
- [10] Donkers R L, Song Y and Murray R W 2004 Substituent effects on the exchange dynamics of ligands on 1.6 nm diameter gold nanoparticles *Langmuir* **20** 4703–7
- [11] Hostetler M J, Templeton A C and Murray R W 1999 Dynamics of place-exchange reactions on monolayer-protected gold cluster molecules *Langmuir* **15** 3782–9
- [12] Magoga M and Joachim C 1997 Conductance and transparency of long molecular wires *Phys. Rev. B* **56** 4722–9
- [13] Tomfohr J K and Sankey O F 2002 Simple estimates of the electron transport properties of molecules *Phys. Status. Solidi b* **233** 59–69
- [14] Salomon A, Cahen D, Lindsay S, Tomfohr J, Engelkes V B and Frisbie C D 2003 Comparison of electronic transport measurements on organic molecules *Adv. Mater.* **15** 1881–90
- [15] Tomfohr J K and Sankey O F 2002 Complex band structure, decay lengths, and fermi level alignment in simple molecular electronic systems *Phys. Rev. B* **65** 245105
- [16] Wang W, Lee T and Reed M A 2005 Electronic transport in molecular self-assembled monolayer devices *Proc. IEEE* **93** 1815–24
- [17] Holmlin R E, Haag R, Chabinyc M L, Ismagilov R F, Cohen A E, Terfort A, Rampi M A and Whitesides G M 2001 Electron transport through thin organic films in metal–insulator–metal junctions based on self-assembled monolayer *J. Am. Chem. Soc.* **123** 5075–85
- [18] Sachs S B, Dudek S P, Hsung R P, Sita L R, Smalley J F, Newton M D, Feldberg S W and Chidsey C E D 1997 Rates of interfacial electron transfer through pi-conjugated spacers *J. Am. Chem. Soc.* **119** 10563–4
- [19] Creager S *et al* 1999 Electron transfer at electrodes through conjugated ‘molecular wire’ bridges *J. Am. Chem. Soc.* **121** 1059–4
- [20] Pettersson K, Wiberg J, Ljungdahl T, Martensson J and Albinsson B 2006 Interplay between barrier width and height in electron tunneling: photoinduced electron transfer in porphyrin-based donor–bridge–acceptor systems *J. Phys. Chem. A* **110** 319–26
- [21] Atienza C, Martin N, Wielopolski M, Haworth N, Clark T and Guldi D M 2006 Tuning electron transfer through p-phenyleneethynylene molecular wires *Chem. Commun.* 3202–4
- [22] Selzer Y, Salomon A and Cahen D 2002 The importance of chemical bonding to the contact for tunneling through alkyl chains *J. Phys. Chem. B* **106** 10432–9